

# High-Dimensional Quantum Eavesdropping: A Hypothetical Attack on BB84 & SSP

Christopher Dunne

December 2, 2023

## Abstract

Quantum key distribution algorithms are considered secure because they leverage quantum phenomena to provide security. As such, eavesdroppers can be detected by analyzing the error rate in the shared key obtained by the parties performing the key exchange. Nevertheless, this paper developed and investigated a novel attack strategy capable of being undetected through error analysis of the shared key. Said attack entails an eavesdropper measuring the quantum channel (i.e., the channel used to transmit quantum particles between two parties) using a higher dimension than that used by the legitimate parties. By measuring a particle in a dimension that spans all possible states in a given quantum key distribution algorithm, the collapsed state of the measured particle should be undetectable when measured in the lower dimension. To analyze the proposed high-dimensional eavesdropping attack, the simulator Cirq was used to model the attack on BB84, a four-dimensional variant of BB84, and the Six-State Protocol. The results of these simulations show the efficiency of this attack, with an eavesdropper being undetectable through quantum bit error rate analysis in each algorithm. This promotes the need for further analysis of the high-dimensional eavesdropping attack on physical hardware and other quantum key distribution algorithms.

# Contents

<b>1</b>	<b>Introduction</b>	<b>4</b>
1.1	Background of Study . . . . .	4
1.2	Problem Statement . . . . .	4
1.3	Significance of Study . . . . .	4
1.4	Nature of Study . . . . .	5
1.5	Conceptual or Theoretical Framework . . . . .	5
1.6	Hypotheses/Research Questions . . . . .	6
1.7	Assumptions and Limitations . . . . .	6
<b>2</b>	<b>Literature Review</b>	<b>7</b>
2.1	History of Quantum Key Distribution Algorithms . . . . .	7
2.2	Research on the Security of QKD . . . . .	7
2.2.1	MitM Attacks on BB84 . . . . .	7
2.2.2	Detection of Eve . . . . .	8
2.3	High-Dimensional Quantum Key Distribution . . . . .	8
<b>3</b>	<b>Methodology</b>	<b>9</b>
3.1	BB84 . . . . .	10
3.1.1	Control Group . . . . .	10
3.1.2	Gate Creation for HD-Eavesdropping . . . . .	10
3.2	HD-BB84 . . . . .	12
3.2.1	Control Group . . . . .	12
3.2.2	Gate Creation for HD-Eavesdropping . . . . .	13
3.3	SSP . . . . .	15
3.3.1	Control Group . . . . .	15
3.3.2	Gate Creation for HD-Eavesdropping . . . . .	16
<b>4</b>	<b>Results</b>	<b>18</b>
<b>5</b>	<b>Discussion</b>	<b>20</b>
<b>6</b>	<b>Conclusion</b>	<b>21</b>
	<b>References</b>	<b>22</b>
<b>A</b>	<b>Reading Qudit Measurements in HD-Eavesdropping</b>	<b>26</b>
<b>B</b>	<b>Conversion Matrices</b>	<b>27</b>

# 1 Introduction

The quantum key distribution (QKD) algorithm BB84 leverages Heisenberg’s uncertainty principle and the no-cloning theorem to provide security and serves as the basis for several other QKD algorithms (Sabani, Savvas, Poulakis, & Makris, 2022). By encoding data in two non-orthogonal quantum states, one creates a secure quantum channel that cannot reliably be read or copied by an eavesdropper without altering it in such a way that will be easily noticed (Bennett & Brassard, 1984). However, this assumes that an eavesdropper is measuring the quantum channel using the same number of dimensions as that used by the legitimate parties. This paper will explore the usage of higher dimensions to eavesdrop BB84 and several variants based on it. This high-dimensional eavesdropping attack was modeled using the quantum simulator Cirq.

## 1.1 Background of Study

Cryptography is the practice of protecting data by hiding its content, preventing unauthorized access, and preventing undetected modification (Franklin et al., 2020; Amellal, Hajjami, Kaushik, Chhabra, & Yadav, 2023). It is utilized by billions of devices to secure sensitive information such as financial and medical records (Shingari & Mago, 2024) and is vital in the operation of cloud computing (Sasikumar & Nagarajan, 2024) and the internet (Liu & Moody, 2024). There are two types of encryption algorithms, symmetric and asymmetric algorithms. Symmetric algorithms use the same key for both encryption and decryption, whereas asymmetric algorithms use different keys for these processes (Sood & Kaur, 2023). Secure key distribution is essential in both types of algorithms.

Key distribution entails the transportation of cryptographic keys and other keying material between a party that has a key and a party that needs a key. This process is critical to ensure the security of both symmetric and asymmetric encryption algorithms (Barker, 2020). Classical key distribution algorithms rely on mathematically difficult to solve problems to provide security, whereas QKD algorithms rely on the fundamental laws of nature (Singh, Singh, & Sreenarayanan, 2022; Lee, Sohn, & Lee, 2022; Bommi, Nalini, Vijayaraj, & Kinol, 2023).

## 1.2 Problem Statement

It is easy to assume that QKD algorithms provide unconditional security due to their leverage of quantum mechanics. Despite this, it is crucial to thoroughly explore all possible attack vectors on an algorithm before implementation. This paper develops and investigates a novel attack strategy that exploits quantum phenomena to eavesdrop on the QKD algorithm BB84 and two of its derivatives.

The Heisenberg uncertainty principle states that it is impossible to measure a particle without altering its state. This is utilized by QKD algorithms to provide security as an eavesdropper will always produce a change in the system (Singh et al., 2022). However, this is reliant on the assumption that the eavesdropper measures the quantum particle in the same number of dimensions as that used by the legitimate parties. This assumption will be challenged by a proposed high-dimensional eavesdropping attack to demonstrate a potential weakness in QKD algorithms that rely on the uncertainty principle to provide security.

## 1.3 Significance of Study

Any algorithm intended to protect devices must undergo rigorous analysis before implementation. The necessity of doing so can be seen in the Supersingular Isogeny Key Encapsulation (SIKE) algorithm, which was a final candidate that the National Institute of Standards and Technology (NIST)

was evaluating for its post-quantum cryptography standards. However, Castryck and Decru demonstrated an attack based on a theorem first proposed in 1997 that was capable of breaking SIKE in approximately 62 minutes using a legacy system (Castryck & Decru, 2023). Before this attack had been demonstrated, SIKE was widely considered to be a secure cryptographic algorithm (Longa, Wang, & Szefer, 2021; Costello, 2021; Stratil, Hasegawa, & Shizuya, 2021).

Another algorithm that NIST was evaluating for its post-quantum security was the Rainbow signature scheme. Rainbow was first proposed in 2005 by Ding and Schmidt and is a multivariate signature scheme based on the unbalanced Oil and Vinegar signature scheme (Ding & Schmidt, 2005). In 2022, Beullens found an attack vector capable of breaking Rainbow in a week on a laptop. To secure the Rainbow algorithm against this attack, one would have to increase the size of the keys and signatures generated. However, doing so would make it less efficient than the Oil and Vinegar algorithm it was built upon. Furthermore, further investigation would still be required to see if the attack could be optimized for the larger key sizes of this modified version of Rainbow (Beullens, 2022).

Cryptographic algorithms are utilized by a wide spectrum of areas such as healthcare, banking, retail, and government entities (Singh et al., 2022; Kose, Coskun, Capa, & Uluoz, 2024). A premature implementation of SIKE or Rainbow before either of these attacks were discovered would have severe consequences for any of said entities. As such, analyzing attack vectors on cryptographic algorithms before mass adoption is important to prevent the loss of vital information and resources.

Finally, multiple regulations require cryptography. Two such regulations are the General Data Protection Regulation (GDPR) and the Health Insurance Portability and Accountability Act (HIPAA). The GDPR is applicable to all organizations that collect personal data in the European Union (Council of the European Union & European Parliament, 2016), whereas HIPAA is applicable solely to sensitive health information of patients in the United States (Office of the Federal Register & National Archives and Records Administration, 1996).

## 1.4 Nature of Study

A novel attack vector on the QKD algorithms BB84, its four-dimensional variant, and the Six-State Protocol (SSP) using an experimental research method will be investigated. The attack vector analyzed involves a higher-dimensional measurement basis than that used by the legitimate parties. The quantum simulator Cirq will be employed to model the QKD algorithms and the proposed attack. Doing so will produce quantitative data in the form of the error introduced by an eavesdropper and how much knowledge said eavesdropper obtains when performing the high-dimensional eavesdropping attack.

## 1.5 Conceptual or Theoretical Framework

Particles can be expressed as a matrix of probabilities that correspond to the likelihood of being measured in a certain axis or state. As per Heisenberg's uncertainty principle, the measurement of a particle can only be certain when its direction coincides with one of the matrix's main axes. When this happens, there will only ever be one state measured. However, if the direction of a particle deviates from one of these main axes, their measurements will have a probable error rate relative to the deviation. Therefore, for each quantum variable, there exists a system of coordinates wherein the probable error ceases to exist for that variable (Heisenberg, 1983/1927).

BB84 leverages this by using two encoding bases that exist in an even superposition between each other, causing a particle in one encoding basis to have a deviation that results in a 50% error rate relative to the other encoding basis. Due to this, when an eavesdropper measures a

particle without knowing its encoding basis, this should result in each intercepted particle having a 25% chance of being measured incorrectly by the legitimate parties when in an environment with no noise (Salas & Barreto, 2024; Alhazmi, Kandel, Sabovik, Matondo-Mvula, & Elleithy, 2023). However, this paper speculates that if an eavesdropper were to represent the particles in a quantum channel whose axes span all possible encoding states used, the error rate produced by the deviation from the main axes should be reduced so long as each axis of the expanded matrix is equivalent to each possible direction a particle in the quantum channel can be.

As mentioned above, the error in quantum particles measured, or quantum bit error rate (QBER), can be used to detect an eavesdropper. As such, the dependent variables of interest will be the QBER produced by an eavesdropper and how much knowledge of the shared keys said eavesdropper obtains. These variables are dependent on the data sent through the quantum channel and the number of encoding bases and/or dimensions used in the QKD algorithm. The encoding bases and the dimension of the particles will be dictated by the QKD algorithm used.

Three algorithms will be examined, BB84, a high-dimensional variant of BB84, and SSP. BB84 uses two encoding bases on a two-dimensional particle (Bennett & Brassard, 1984), whereas its high-dimensional variant uses two encoding bases on a four-dimensional particle (Bechmann-Pasquinucci & Tittel, 2000). The final algorithm, SSP, uses three encoding bases on a two-dimensional particle (Bruß, 1998). These algorithms are further discussed in Sections 2 and 3.

## 1.6 Hypotheses/Research Questions

This experimental study will test the following hypotheses:

**Hypothesis 1.** When an eavesdropper uses a high dimensional measurement basis to measure the quantum channel being used to perform BB84 or its variants that rely on the same principle, the produced QBER will be minimal. As such, an analysis of the QBER would not be a valid means of detecting this attack.

**Hypothesis 2.** Given Hypothesis 1, this can be mitigated by using a high-dimensional QKD (HD-QKD) variant of BB84 and its variants, or by using more encoding bases. Doing so should increase the number of dimensions an eavesdropper must use ( $d_e$ ) to Equation 1, wherein  $d_{ab}$  is the dimension of the quantum particle used to transmit data and  $b$  is the number of encoding/decoding bases used by the legitimate parties.

$$d_e = d_{ab} * b \tag{1}$$

## 1.7 Assumptions and Limitations

Without access to physical hardware, the quantum simulator Cirq was used to test the hypotheses. Due to this, it must be assumed that a high-dimensional eavesdropping attack is physically possible. Furthermore, the assumption that no noise was present also had to be made due to time constraints. Cirq natively supports modeling noise on two-dimensional quantum particles and provides the resources necessary to define custom logic that models noise on quantum particles with a higher dimension. However, doing so for complex experiments requires the definition of a custom `NoiseModel` subclass (Cirq Developers, 2024). Creating this subclass for each test proved to be too time-consuming given a limited time frame.

## 2 Literature Review

### 2.1 History of Quantum Key Distribution Algorithms

QKD protocols are key distribution algorithms that leverage quantum mechanics to secure and share secret keys using a quantum channel (James, Laschet, Ramacher, & Torresetti, 2023). The first such protocol, BB84, was proposed in 1984 by Charles Bennett and Gilles Brassard (Sabani et al., 2022).

When using BB84, the sender encodes classical data using photons that serve as quantum bits, or qubits. This is accomplished by polarizing photons in one of two different bases before transmitting them through a quantum channel. The receiver then must guess which basis was used when measuring said photons (Singh et al., 2022).

In 1991, Artur Ekert proposed the QKD protocol E91. This algorithm operates by sending pairs of entangled photons through a quantum channel, with entanglement being defined as two or more particles that cannot be measured as individual independent states (Djordjevic & Nafria, 2024). Entanglement is utilized by E91 to provide security as entangled particles should produce a Clauser-Horne-Shimony-Holt (CHSH) correlation value of  $-2\sqrt{2}$  when undisturbed. As such, a CHSH correlation value that differs from  $-2\sqrt{2}$  indicates a lack of entanglement and the presence of an eavesdropper (Ekert, 1991).

BB84 was expanded upon by Charles Bennett in 1992, presenting a new QKD algorithm. This algorithm, B92, is a variant of BB84 that encodes classical data using two states as opposed to four. Instead of an encoding basis being randomly selected for each bit, the value being encoded determines which basis to use (Bennett, 1992).

Another QKD algorithm, SSP, was defined by Bruß in 1998 and further investigated by Bechmann-Pasquinucci and Gisin in 1999. SSP is a variant of BB84 that uses a third encoding basis conjugate to the rectilinear and diagonal bases of BB84. Doing so increases the QBER produced by an eavesdropper at the cost of an increase of discarded particles. This is because two legitimate parties will only have a one in three chance of using the same encoding and decoding basis (Bruß, 1998).

Finally, in 2004, a variant of BB84 was defined titled SARG04. This algorithm was designed to be secure against photon-number-splitting (PNS) attacks. The PNS attack exploits implementations of QKD protocols that use weak light pulses, as light pulses contain many photons. The attack operates by having an eavesdropper splitting off a single photon from the signal pulse, enabling the measurement of the quantum channel without the introduction of noise (Sabani et al., 2022). SARG04 protects against this attack by altering how parties determine which encoding bases were used for each qubit. Instead of announcing the basis used on a classical channel, a pair of non-orthogonal states are sent via the quantum channel. This requires an eavesdropper to split off more photons from the quantum channel when performing a PNS attack, making their detection easier (Scarani et al., 2004).

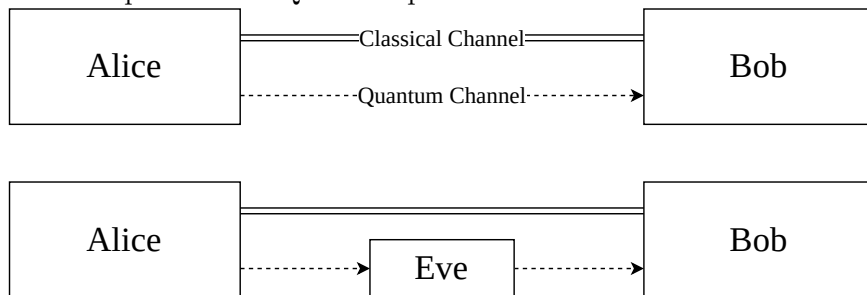
### 2.2 Research on the Security of QKD

#### 2.2.1 MitM Attacks on BB84

Most research on the security of QKD algorithms has been centered on BB84's ability to detect an eavesdropper performing a Man-in-the-Middle (MitM), or intercept-resend, attack. Such attacks aim to obtain the encryption key being shared without the knowledge of the intended recipients (Jawad, Mahmood, & Hameed, 2023). This can be achieved by cutting the quantum channel between Alice and Bob before connecting the severed ends to a pair of QKD devices capable of measuring and encoding photons (Alhazmi et al., 2023; Liliana, 2019). This process is demonstrated

in Figure 1.

Figure 1: A depiction of a QKD setup both with and without an eavesdropper.



To measure the intercepted photons, Eve must follow the same steps as Bob, selecting a random decoding basis for each photon before measurement. Eve must then encode their measurements in its respective basis before sending them to Bob (Huang, Wang, Wang, Li, & Huang, 2009).

### 2.2.2 Detection of Eve

If Eve randomly chooses the same base as Alice, the state of the electron will not be altered. However, if Eve measures the particle using a different base, the particle will randomly collapse into either a 1 or 0 with equal probability. Because of this, Bob has a 25% chance of measuring each intercepted photon incorrectly when in an environment with no noise. As such, the probability of Eve being detected  $P_d$  given  $K$  qubits are given by the formula  $P_d = 1 - (3/4)^K$  (Salas & Barreto, 2024; Alhazmi et al., 2023).

## 2.3 High-Dimensional Quantum Key Distribution

Qubits only use two states of a physical property to store and process information. However, many such properties have multiple usable states. This can include properties such as particle frequency, energy level, spin state (Wang, Hu, Sanders, & Kais, 2020) and orbital angular momentum (OAM) (Zi, Li, & Sun, 2023). Quantum bits that use these additional dimensions are called qudits. This can be leveraged by HD-QKD to encode data as qudits as opposed to qubits, often increasing noise resilience (Müller, Bacco, Oxenløwe, & Forchhammer, 2023). Bechmann-Pasquinucci and Tittel demonstrated how qudits could be utilized in QKD algorithms by defining a four-dimensional variant of BB84 in 2000. This was achieved by redefining the encoding bases used by BB84 to account for the use of four-dimensional qudits, with each qudit representing two bits. Most research on HD-QKD algorithms have analyzed high-dimensional variants of BB84, showing that HD-QKD results in greater key efficiency as well as an increase in QBER when an eavesdropper is present (Liliana, 2019; Zahidy et al., 2024).

An example of the security offered by HD-QKD can be seen in their resistance to quantum cloning attacks. QKD algorithms rely on the no-cloning theorem to provide security (Sabani et al., 2022), which states that it is impossible for one to perfectly copy a quantum state without altering it (Wootters & Zurek, 1982). Despite this, the creation of imperfect copies of quantum states is possible using quantum cloning machines (Idan & Didi, 2024; Iqbal, Ahmadian, Velasco, & Ruiz, 2023).

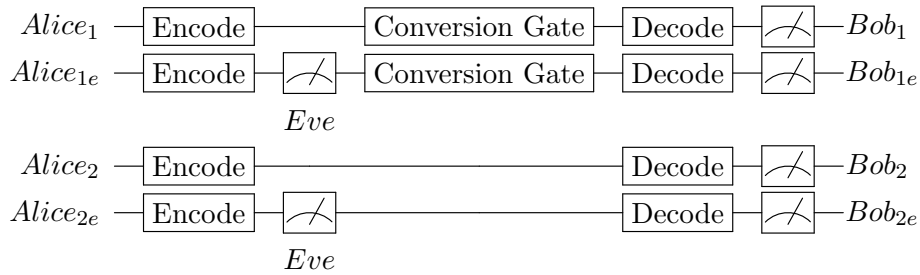
Bouchard, Fickler, Boyd, and Karimi (2017) explored the use of such a machine to perform a MitM attack on BB84 in a paper titled “High-dimensional quantum cloning and applications to quantum hacking”. It detailed a high-dimensional universal quantum cloning machine (UQCM)

capable of creating imperfect clones of the OAM states of photons. This was achieved using two input qubits, the first being the qubit sent between Alice and Bob, and the second being a qubit in an even superposition between all  $d$  dimensions of the first qubit. By passing both photons through a 50:50 beam splitter, they will exit said beam splitter in a similar, if not identical, state due to their bosonic nature. The UQCM was used to attack both high-dimensional and standard versions of BB84, finding that the high-dimensional protocol made an eavesdropper’s presence clearly visible and demonstrating the improved security of HD-QKD compared to their lower dimensional variants.

### 3 Methodology

Key exchanges were performed between two parties, Alice and Bob. When present, the eavesdropper is referred to as Eve. An unmodified version, or control group, of each QKD algorithm was analyzed alongside the impacts of Eve when performing a MitM attack. In addition to the control group, two different means of simulating high-dimensional eavesdropping, **Scenario 1** and **Scenario 2**, were tested. This is because Cirq cannot measure qudits in a dimension different from said qudits dimensions (Cirq Developers, 2024). To account for this, **Scenario 1** converts the high-dimensional qudit encoded by Alice to a lower-dimensional qudit whose dimensions are equal to that of the algorithm’s control group. **Scenario 2** circumvented this limitation by having Bob measure the high-dimensional qudit and altering the resulting binary values to reflect their expected values given the state measured. Figure 2 depicts the logic for **Scenario 1** and **Scenario 2**.

Figure 2: The gates used in **Scenario 1** (denoted by 1) and **Scenario 2** (denoted by 2).



Cirq measures qudits in a range of 0 to  $d - 1$ , where  $d$  is the dimensions of the qudit. These states should correlate to a binary value and its corresponding encoding basis. For example, the qudit states when testing BB84 correlated to the values in Equation 2.

$$\begin{aligned}
 |0\rangle &= 0 \text{ encoded in the rectilinear basis} \\
 |1\rangle &= 0 \text{ encoded in the diagonal basis} \\
 |2\rangle &= 1 \text{ encoded in the rectilinear basis} \\
 |3\rangle &= 1 \text{ encoded in the diagonal basis}
 \end{aligned} \tag{2}$$

Given these states, Bob can replace measurements of two with one and change measurements of one and three to a random bit value. Doing so models the expected behavior of a qubit when represented with a four-dimensional qudit. These alterations, alongside the corresponding binary value of the states measured by Eve, can be seen in Appendix A.

The high-dimensional gate variants were prepended with “Qid” and defined using matrices. The states of a  $d$ -dimensional qudit can be represented by a set of orthonormal state vectors as shown in Equation 3, wherein  $\alpha_d$  is the probability of measuring  $|d\rangle$  and  $|\alpha_0|^2 + |\alpha_1|^2 \dots + |\alpha_{d-1}|^2 = 1$  (Wang et al., 2020).

$$|\alpha\rangle = \alpha_0|0\rangle + \alpha_1|1\rangle + \dots + \alpha_{d-1}|d-1\rangle = \begin{pmatrix} \alpha_0 \\ \alpha_1 \\ \vdots \\ \alpha_{d-1} \end{pmatrix} \quad (3)$$

Quantum gates can also be represented as a matrix whose values correspond to the probability of measuring a given state given an input vector (Spranger, Grimaila, & Hodson, 2023).

When applying a quantum gate to  $n$  qudits, one must first calculate the joint states of said qudits (Spranger et al., 2023). Consequently, applying a gate to multiple qudits with different dimensions will produce a matrix whose size is the sum of the squares of each qudit’s dimensions. For example, a quantum gate that operates on an eight-dimensional qudit, a two-dimensional qubit, and a four-dimensional qudit will result in a matrix of size  $64^2$ .

### 3.1 BB84

#### 3.1.1 Control Group

BB84 relies on two conjugate bases, the rectilinear and diagonal basis. The use of conjugate bases ensures that when a particle is in a specific state of one basis, measuring said particle in the other basis results in a random output. The rectilinear basis is defined as a particle with a polarization of either  $0^\circ$  or  $90^\circ$ , whereas the diagonal basis is defined as a particle with a polarization of either  $45^\circ$  or  $135^\circ$  (Bennett & Brassard, 1984).

To perform a key exchange via BB84, Alice must first generate a random key that will be encoded and shared with Bob and choose an encoding basis for each bit of the key (Bennett & Brassard, 1984). A Hadamard-gate (H-gate) can be used to encode or decode a qubit in the diagonal basis. The properties of the H-gate are provided in Equation 4. An X-gate is applied to a qubit before transmission if a binary 1 is being encoded. To decode the quantum channel, Bob must choose a random measurement basis for each qubit received. When present, Eve follows the same procedure as Bob (Saeed, Sattar, Durad, & Haider, 2022).

$$\begin{aligned} H|0\rangle &= \frac{1}{\sqrt{2}}(|0\rangle + |1\rangle) = |+\rangle \\ H|1\rangle &= \frac{1}{\sqrt{2}}(|0\rangle - |1\rangle) = |-\rangle \end{aligned} \quad (4)$$

Once Bob has received and measured all qubits sent by Alice, the two generate a sifted key. This is accomplished by sharing the encoding and decoding basis used for each qubit, and discarding bits measured in different bases (Bennett & Brassard, 1984). The two parties then check for the presence of an eavesdropper by comparing a number of bits in the sifted key. Without an eavesdropper or noise, all compared bits of the sifted key should be identical (Bennett & Brassard, 1984; Saeed et al., 2022).

#### 3.1.2 Gate Creation for HD-Eavesdropping

The states of Eve’s qudit are given in Equation 5. Since Cirq is unable to measure qudits using a different dimension, high-dimensional variants of the X- and H-gate had to be defined that would

change the state of a qudit based on how their qubit equivalent would normally affect a qubit. In addition to this, **Scenario 1** required the creation of several additional gates used to convert a four-dimensional qudit to a single qubit.

$$\begin{aligned}
 |0\rangle &= |0\rangle \\
 |1\rangle &= |+\rangle \\
 |2\rangle &= |1\rangle \\
 |3\rangle &= |-\rangle
 \end{aligned} \tag{5}$$

**Qid-X<sub>1</sub>**. The X-gate is the equivalent of a classical bit flip, and has the properties outlined in Equation 6 (Nielsen & Chuang, 2010). A high-dimensional variant of the X-gate that reflects this is provided in Equation 7.

$$X \begin{pmatrix} \alpha \\ \beta \end{pmatrix} = \begin{pmatrix} \beta \\ \alpha \end{pmatrix} \tag{6}$$

$$\begin{aligned}
 X|0\rangle &= |2\rangle \\
 X|1\rangle &= |1\rangle \\
 X|2\rangle &= |0\rangle \\
 X|3\rangle &= -|3\rangle
 \end{aligned} \tag{7}$$

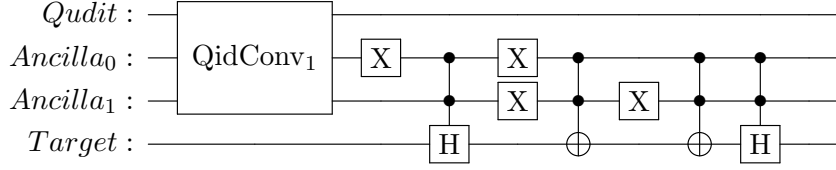
**Qid-H<sub>1</sub>**. Equation 8 lists the properties of the H-gate (Qiskit contributors, 2023). A high-dimensional variant of the H-gate that reflects this is provided in Equation 9.

$$\begin{aligned}
 H|0\rangle &= |+\rangle \\
 H|1\rangle &= |-\rangle \\
 H|+\rangle &= |0\rangle \\
 H|-\rangle &= |1\rangle
 \end{aligned} \tag{8}$$

$$\begin{aligned}
 H|0\rangle &= |1\rangle \\
 H|1\rangle &= |0\rangle \\
 H|2\rangle &= |3\rangle \\
 H|3\rangle &= |2\rangle
 \end{aligned} \tag{9}$$

**BB84 Conversion Gate.** A conversion gate for BB84 was used in **Scenario 1** to convert a four-dimensional qudit to a two-dimensional qubit. Figure 3 depicts the logic for this gate, wherein **QidConv<sub>1</sub>** is a unitary that maps a qudit to two qubits that store the encoding basis and encoded value. The matrix for this gate can be seen in Appendix B.

Figure 3: BB84 conversion gate.



## 3.2 HD-BB84

### 3.2.1 Control Group

In 2000, Bechmann-Pasquinucci and Tittel proposed a four-dimensional variant of BB84 that uses two encoding bases on four-dimensional qudits. They defined the first basis, the  $\psi$ -basis, as an arbitrarily chosen set of values given in Equation 10, alongside their corresponding binary value.

$$\begin{aligned}
 |\psi_\alpha\rangle &= 00 \\
 |\psi_\beta\rangle &= 01 \\
 |\psi_\gamma\rangle &= 10 \\
 |\psi_\delta\rangle &= 11
 \end{aligned} \tag{10}$$

To create a symmetric protocol, the second ( $\phi$ ) basis, had to satisfy the criteria outlined in Equation 11.

$$\begin{aligned}
 |\langle\psi_i|\psi_j\rangle| &= \phi_{ij} \\
 |\langle\psi_i|\phi_j\rangle| &= 1/2
 \end{aligned} \tag{11}$$

Multiple bases exist which fulfill these requirements, but Bechmann-Pasquinucci and Tittel opted to use the basis Equation 12.

$$\begin{aligned}
 |\phi_\alpha\rangle &= \frac{1}{2}(|\psi_\alpha\rangle + |\psi_\beta\rangle + |\psi_\gamma\rangle + |\psi_\delta\rangle) \\
 |\phi_\beta\rangle &= \frac{1}{2}(|\psi_\alpha\rangle - |\psi_\beta\rangle + |\psi_\gamma\rangle - |\psi_\delta\rangle) \\
 |\phi_\gamma\rangle &= \frac{1}{2}(|\psi_\alpha\rangle - |\psi_\beta\rangle - |\psi_\gamma\rangle + |\psi_\delta\rangle) \\
 |\phi_\delta\rangle &= \frac{1}{2}(|\psi_\alpha\rangle + |\psi_\beta\rangle - |\psi_\gamma\rangle - |\psi_\delta\rangle)
 \end{aligned} \tag{12}$$

However, when trying to use this  $\phi$ -basis, the results differed from the expected output. Equation 13 details the behavior that occurred when both Alice and Bob used the  $\phi$ -basis to encode and decode the quantum channel.

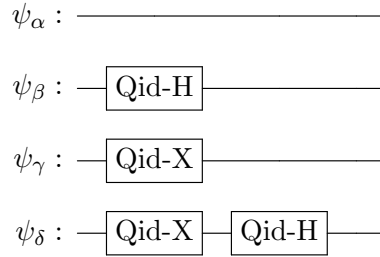
$$\begin{aligned}
 \phi^2|\psi_\alpha\rangle &= |\psi_\alpha\rangle \\
 \phi^2|\psi_\beta\rangle &= |\psi_\delta\rangle \\
 \phi^2|\psi_\gamma\rangle &= |\psi_\beta\rangle \\
 \phi^2|\psi_\delta\rangle &= |\psi_\gamma\rangle
 \end{aligned} \tag{13}$$

Such behavior meant that Bob would measure a different value than that sent by Alice even when the two used the  $\phi$ -basis. As such, the  $\phi$ -basis was redefined to be that in Equation 14.

$$\begin{aligned}
 |\phi_\alpha\rangle &= \frac{1}{2}(|\psi_\alpha\rangle + |\psi_\beta\rangle + |\psi_\gamma\rangle + |\psi_\delta\rangle) \\
 |\phi_\beta\rangle &= \frac{1}{2}(|\psi_\alpha\rangle + |\psi_\beta\rangle - |\psi_\gamma\rangle - |\psi_\delta\rangle) \\
 |\phi_\gamma\rangle &= \frac{1}{2}(|\psi_\alpha\rangle - |\psi_\beta\rangle + |\psi_\gamma\rangle - |\psi_\delta\rangle) \\
 |\phi_\delta\rangle &= \frac{1}{2}(|\psi_\alpha\rangle - |\psi_\beta\rangle - |\psi_\gamma\rangle + |\psi_\delta\rangle)
 \end{aligned}
 \tag{14}$$

Similar to BB84, the high-dimensional variant created to model high-dimensional eavesdropping entails Alice encoding a photon before applying the randomly chosen encoding basis. As shown in Equation 10, there are four states in each encoding basis wherein each state represents two bits instead of one bit. Consequently, half as many particles is needed compared to BB84. Same as in BB84, Alice must first encode a quantum particle in the  $\psi$ -basis before applying the  $\phi$ -basis. To account for this, an  $\alpha$ -,  $\beta$ -,  $\gamma$ -, and  $\delta$ -gate were defined using the quantum gates required to perform high-dimensional eavesdropping on BB84. These gates are illustrated in Figure 4.

Figure 4:  $\psi$  Gates



The process of performing a MitM attack are identical to that in BB84, with the only difference being the usage of the  $\psi$ - and  $\phi$ -basis instead of the rectilinear and diagonal basis. It should also be noted that, when creating the sifted key, bits are discarded in two-bit chunks. In other words, two bits are either kept or discarded depending on whether Alice and Bob used the same or different encoding bases respectively (Bechmann-Pasquinucci & Tittel, 2000).

### 3.2.2 Gate Creation for HD-Eavesdropping

The states of Eve's qudit when performing the high-dimensional eavesdropping attack are given in Equation 15. Once again, high-dimensional variants of the gates used to perform this high-dimensional BB84 variant had to be defined alongside gates to convert the eight-dimensional qudit to a four-dimensional qudit.

$$\begin{aligned}
|0\rangle &= |\psi_\alpha\rangle \\
|1\rangle &= |\phi_\alpha\rangle \\
|2\rangle &= |\psi_\beta\rangle \\
|3\rangle &= |\phi_\beta\rangle \\
|4\rangle &= |\psi_\gamma\rangle \\
|5\rangle &= |\phi_\gamma\rangle \\
|6\rangle &= |\psi_\delta\rangle \\
|7\rangle &= |\phi_\delta\rangle
\end{aligned} \tag{15}$$

**Qid- $\psi$  and Qid- $\phi$  Gates.** Table 1 depicts the high-dimensional variants of the gates used to manipulate qudits in the  $\psi$  basis, alongside the high-dimensional variant of the  $\phi$ -gate.

Table 1: The results of a given input state to their corresponding output state when a high-dimensional variant of the  $\alpha$ -,  $\beta$ -,  $\gamma$ -,  $\delta$ -, or  $\phi$ -gate is applied.

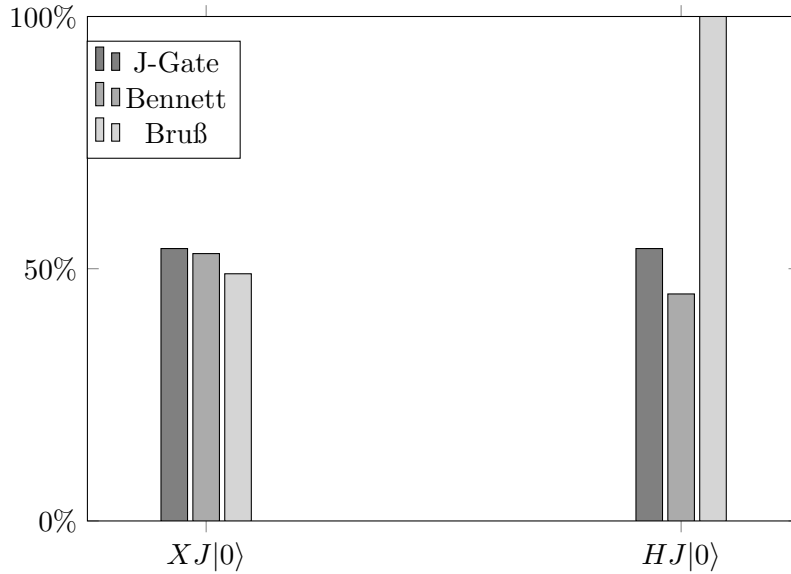
Input State	Qid- $\alpha$	Qid- $\beta$	Qid- $\gamma$	Qid- $\delta$	Qid- $\phi$
$ 0\rangle$	$ 0\rangle$	$ 2\rangle$	$ 4\rangle$	$ 6\rangle$	$ 1\rangle$
$ 1\rangle$	$ 1\rangle$	$ 3\rangle$	$ 5\rangle$	$ 7\rangle$	$ 0\rangle$
$ 2\rangle$	$ 2\rangle$	$ 0\rangle$	$ 6\rangle$	$ 4\rangle$	$ 3\rangle$
$ 3\rangle$	$ 3\rangle$	$ 1\rangle$	$ 7\rangle$	$ 5\rangle$	$ 2\rangle$
$ 4\rangle$	$ 4\rangle$	$ 6\rangle$	$ 0\rangle$	$ 2\rangle$	$ 5\rangle$
$ 5\rangle$	$ 5\rangle$	$ 7\rangle$	$ 1\rangle$	$ 3\rangle$	$ 4\rangle$
$ 6\rangle$	$ 6\rangle$	$ 4\rangle$	$ 2\rangle$	$ 0\rangle$	$ 7\rangle$
$ 7\rangle$	$ 7\rangle$	$ 5\rangle$	$ 3\rangle$	$ 1\rangle$	$ 6\rangle$

**HD-BB84 Conversion Gate.** A conversion gate for the four-dimensional variant of BB84 was used in **Scenario 1** to convert an eight-dimensional qudit to a four-dimensional qudit. The logic for this gate can be seen in Figure 5. The  $\text{QidConv}_2$  gate maps the states of an eight-dimensional qudit to a four-dimensional qudit and a two-dimensional ancilla qubit. The qubit is used to determine what encoding basis to apply using a conditional  $\phi$ -gate ( $C\phi$ ), while the four-dimensional qudit will be the value measured by Bob. The unitary for  $\text{QidConv}_2$  can be seen in Appendix B.

Figure 5: HD-BB84 conversion gate.



Figure 6: The percentage of 0's measured after an X-gate or H-gate has been applied to 100 qubits encoded in the y-axis given the states defined in this paper, Bennett and Brassard, and Bruß.



### 3.3 SSP

#### 3.3.1 Control Group

The two axes BB84 uses to encode qubits are the z- and x-axis for the rectilinear and diagonal basis respectively. However, Bennett and Brassard provided another possible basis conjugate to both the rectilinear and diagonal bases that could be used instead. This basis exists on the y-axis and consists of the circular polarizations Equation 16 (Bennett & Brassard, 1984).

$$|i\rangle = \frac{1}{\sqrt{2}} \begin{pmatrix} 1 \\ i \end{pmatrix} \quad |-i\rangle = \frac{1}{\sqrt{2}} \begin{pmatrix} i \\ 1 \end{pmatrix} \quad (16)$$

Bruß expanded upon this in 1998 with SSP, a variant of BB84 that uses the x-, y-, and z-axes, and was further investigated by Bechmann-Pasquinucci and Gisin in 1999. Though the y-axis for SSP was redefined to be that in Equation 17.

$$|i\rangle = \frac{1}{\sqrt{2}} \begin{pmatrix} 1 \\ i \end{pmatrix} \quad |-i\rangle = \frac{1}{\sqrt{2}} \begin{pmatrix} 1 \\ -i \end{pmatrix} \quad (17)$$

However, neither basis could be used. For a basis to be secure, measurement on a different basis should result in a random value. As such, when an X- or H-gate is applied to a particle encoded in the y-axis, the results measured should be random. As can be seen in Figure 6, the states defined by Bennett and Brassard meet said criterion, whereas the states provided by Bruß do not.

Another criterion that must be met is that applying the basis twice should result in the original value when measured. As can be seen in Equation 18, the states provided by Bennett and Brassard do not achieve this. When applying their basis twice, it would result in the inverse of the encoded value.

$$\frac{1}{\sqrt{2}} \begin{pmatrix} 1 & i \\ i & 1 \end{pmatrix}^2 = \begin{pmatrix} 0 & i \\ i & 0 \end{pmatrix} \quad (18)$$

As such, the circular polarization had to be redefined to Equation 19. The corresponding gate to apply this basis was defined as the J-gate<sup>1</sup>. As can be seen in Figure 6 and Equation 20, this basis satisfies both criteria.

$$|i\rangle = \frac{1}{\sqrt{2}} \begin{pmatrix} i \\ 1 \end{pmatrix} \quad |-i\rangle = \frac{1}{\sqrt{2}} \begin{pmatrix} -1 \\ -i \end{pmatrix} \quad (19)$$

$$\frac{1}{\sqrt{2}} \begin{pmatrix} i & -1 \\ 1 & -i \end{pmatrix}^2 = \begin{pmatrix} -1 & 0 \\ 0 & -1 \end{pmatrix} \quad (20)$$

### 3.3.2 Gate Creation for HD-Eavesdropping

The states of Eve's qudits are given in Equation 21. Same as with BB84 and its high-dimensional variant, high-dimensional X-, H-, and J-gates had to be defined in addition to gates that convert a six-dimensional qudit to a qubit.

$$\begin{aligned} |0\rangle &= |0\rangle \\ |1\rangle &= |+\rangle \\ |2\rangle &= |i\rangle \\ |3\rangle &= |1\rangle \\ |4\rangle &= |-\rangle \\ |5\rangle &= |-i\rangle \end{aligned} \quad (21)$$

**Qid-X<sub>2</sub>-, H<sub>2</sub>-, and J-Gates.** The high-dimensional variants of the X- and H-gates were obtained by modifying those created when testing BB84. The results of applying an X- or H-gate to a J-gate are displayed in Equation 22,

$$\begin{aligned} X|i\rangle &= -|-i\rangle & H|i\rangle &= |i\rangle \\ X|-i\rangle &= -|i\rangle & H|-i\rangle &= |-i\rangle \end{aligned} \quad (22)$$

and the J-gate has the properties depicted in Equation 23. Interestingly, the Qid-J-gate unitary ended up being equal to the negative Qid-X-gate with reversed columns and vice versa, as seen in Equation 24.

$$\begin{aligned} J|0\rangle &= |i\rangle \\ J|1\rangle &= |-i\rangle \\ J|+\rangle &= |-\rangle \\ J|-\rangle &= |+\rangle \\ J|i\rangle &= -|0\rangle \\ J|-i\rangle &= -|1\rangle \end{aligned} \quad (23)$$

---

<sup>1</sup>Y is commonly associated with the Pauli-Y gate and I is commonly associated with the Identity gate (Qiskit contributors, 2023). As such, J was selected because *j* is a commonly used alternative for *i* (Du, 2023).

$$QidX_2 = \begin{pmatrix} 0 & 0 & 0 & 1 & 0 & 0 \\ 0 & 1 & 0 & 0 & 0 & 0 \\ 0 & 0 & 0 & 0 & 0 & -1 \\ 1 & 0 & 0 & 0 & 0 & 0 \\ 0 & 0 & 0 & 0 & -1 & 0 \\ 0 & 0 & -1 & 0 & 0 & 0 \end{pmatrix} \quad QidJ = \begin{pmatrix} 0 & 0 & -1 & 0 & 0 & 0 \\ 0 & 0 & 0 & 0 & -1 & 0 \\ 1 & 0 & 0 & 0 & 0 & 0 \\ 0 & 0 & 0 & 0 & 0 & -1 \\ 0 & 1 & 0 & 0 & 0 & 0 \\ 0 & 0 & 0 & 1 & 0 & 0 \end{pmatrix} \quad (24)$$

**SSP Conversion Gate.** A gate that converts a six-dimensional qudit to a two-dimensional qubit when modeling SSP is depicted in Figure 7. The gate uses a three-dimensional qudit, or qutrit, to determine the encoding basis to apply to the qubit using a conditional Hadamard/J-gate (CHJ-gate). Appendix B and Equation 25 depict the unitary for  $QidConv_3$  and the CHJ-gate respectively. As is demonstrated in Equation 25, an H-gate is applied if the qutrit is in the state  $|1\rangle$ , whereas a J-gate is applied if it is in the state  $|2\rangle$ .

Figure 7: SSP conversion gate.



$$\begin{pmatrix} 1 & 0 & 0 & 0 & 0 & 0 \\ 0 & 1 & 0 & 0 & 0 & 0 \\ 0 & 0 & \frac{1}{\sqrt{2}} & \frac{1}{\sqrt{2}} & 0 & 0 \\ 0 & 0 & \frac{1}{\sqrt{2}} & -\frac{1}{\sqrt{2}} & 0 & 0 \\ 0 & 0 & 0 & 0 & \frac{i}{\sqrt{2}} & -\frac{1}{\sqrt{2}} \\ 0 & 0 & 0 & 0 & \frac{1}{\sqrt{2}} & -\frac{i}{\sqrt{2}} \end{pmatrix} \quad (25)$$

## 4 Results

Tables 2, 3, and 4 list the results of each scenario when performed 25 times. This includes the size of the sifted key compared to the total amount of bits sent between Alice and Bob alongside the average QBER both with and without the presence of Eve. They also list Eve’s knowledge of Alice’s and Bob’s sifted key. Finally, they display the percentage of tests that produced sifted keys identical to that created in the control group without the presence of Eve (Matches). Results measured in Eve’s presence are denoted by  $E$ .

A match of 100% in **Scenario 1** and **Scenario 2** without the presence of Eve indicates that the model accurately reflects the expected behavior of the associated QKD algorithm. A match of 100% in **Scenario 1** and **Scenario 2** with the presence of Eve indicates that the high-dimensional eavesdropping attack produced no QBER in any test. The average QBER produced by Eve in each scenario is illustrated in Figure 8.

Table 2: Results from simulating BB84.

	Key Size	QBER	Alice Knowledge	Bob Knowledge	Matches
Control	109 (54.5%)	0%			
Scenario 1	109 (54.5%)	0%			100%
Scenario 2	109 (54.5%)	0%			100%
Control $_E$	109 (54.5%)	25.03%	74.86%	75.96%	0%
Scenario 1 $_E$	109 (54.5%)	0%	100%	100%	100%
Scenario 2 $_E$	109 (54.5%)	0%	100%	100%	100%

Table 3: Results from simulating HD-BB84.

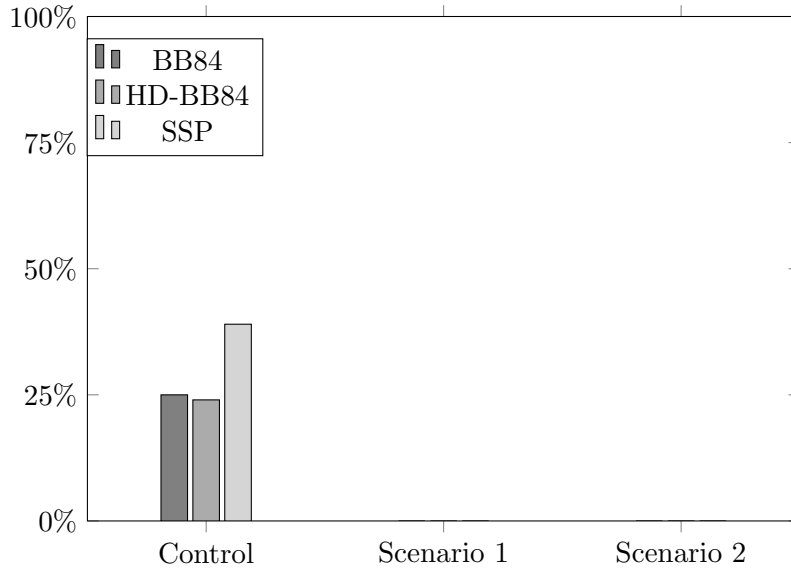
	Key Size	QBER	Alice Knowledge	Bob Knowledge	Matches
Control	78 (39%)	0%			
Scenario 1	78 (39%)	0%			100%
Scenario 2	78 (39%)	0%			100%
Control $_E$	78 (39%)	23.69%	76.26%	77.9%	0%
Scenario 1 $_E$	78 (39%)	0%	100%	100%	100%
Scenario 2 $_E$	78 (39%)	0%	100%	100%	100%

Table 4: Results from simulating SSP.

	Key Size	QBER	Alice Knowledge	Bob Knowledge	Matches
Control	69 (34.5%)	0%			
Scenario 1	69 (34.5%)	0%			100%
Scenario 2	69 (34.5%)	0%			100%
Control $_E$	69 (34.5%)	38.55%	71.42%	60.7%	0%
Scenario 1 $_E$	69 (34.5%)	0%	100%	100%	100%
Scenario 2 $_E$	69 (34.5%)	0%	100%	100%	100%

The average QBER produced by Eve in the control group closely matches the expected QBER of the control’s corresponding algorithm. BB84 and its high-dimensional variant should both pro-

Figure 8: The average QBER of BB84, its high-dimensional variant, and SSP when an eavesdropper is present.



duce a QBER of approximately 25% while Eve is present (Bennett & Brassard, 1984; Bechmann-Pasquinucci & Tittel, 2000), whereas SSP should produce a QBER of approximately 33% (Bechmann-Pasquinucci & Gisin, 1999). These results demonstrate that the presence of Eve did not introduce any QBER when using a high-dimensional eavesdropping strategy, thus supporting the hypothesis that the use of a high-dimensional basis by Eve will produce a minimal QBER when eavesdropping BB84 and its variants.

## 5 Discussion

Based on the results of the simulations, a potential attack vector exists for QKD algorithms that rely on Heisenberg’s uncertainty principle to provide security. If an eavesdropper were to measure the quantum channel in a number of dimensions equal to that in Equation 1, no noise should be introduced by the eavesdropper. A means of mitigating this would be the use of additional dimensions and encoding bases, thus increasing the number of dimensions an eavesdropper would need to measure with a single sensor. Indeed, the high-dimensional variant of BB84 would require Eve to use an eight-dimensional sensor, whereas SSP would require a six-dimensional sensor. However, this causes a reduced key efficiency, as Alice and Bob will be more likely to choose an incorrect encoding basis (Bechmann-Pasquinucci & Tittel, 2000; Bechmann-Pasquinucci & Gisin, 1999).

Alternatively, QKD algorithms that rely on entanglement, such as E91, may not be affected by this attack. E91 provides security by analyzing how entangled particles are. This is achieved using the CHSH correlation value of the results measured by Alice and Bob. A CHSH correlation value that differs from  $-2\sqrt{2}$  indicates a lack of entanglement and the presence of an eavesdropper (Ekert, 1991).

It should also be noted that this assumes the physical possibility of a high-dimensional eavesdropping attack. In addition to this, the tests performed could not account for natural noise that may exist in quantum channels. A number of external sources of noise exist that can occur without the presence of Eve, including decoherence and relaxation. Decoherence occurs when a quantum particle spontaneously loses its state, while relaxation occurs when a particle loses energy. Both sources of error are more likely to occur over time. As such, qubits are limited by their lifespan.

Another source of noise can be that caused by erroneous gate operations and measurements. Quantum gates cause gate errors when they fail to properly alter the state of a particle, whereas a measurement error occurs when the incorrect state is measured (Saki et al., 2021).

While these factors could not be analyzed given time constraints and a lack of hardware, they could potentially introduce unexpected behavior. The qubits on the quantum channel would have a shorter lifespan when in the presence of Eve since they would have to travel a shorter distance from Alice to Eve and from Eve to Bob. This is because once Eve intercepts a qubit from Alice, Eve must then create a new qubit to be sent to Bob. Therefore, the shorter lifespan of qubits should reduce the noise caused from decoherence and relaxation. However, Eve may still produce noise depending on how accurate their measurements and gate operations are. While this promotes the need to perform further research using physical hardware, it is unlikely that the sources of noise provided and reduced by Eve would be significant enough to detect.

## 6 Conclusion

A novel high-dimensional eavesdropping attack was developed and performed on QKD algorithms that rely on Heisenberg's uncertainty principle to provide security. Based on simulated attacks on BB84, a high-dimensional variant of BB84, and SSP, it was demonstrated that a high-dimensional eavesdropping attack will produce zero QBER in a quantum channel. For this attack to be performed, an eavesdropper must measure the quantum channel as a  $d$  dimensional qudit, wherein  $d$  is determined by the dimensions of the quantum channel and number of encoding bases used. The number of dimensions an eavesdropper must use is given in Equation 1.

This demonstrates a here-to-fore unexplored vulnerability of QKD algorithms. Such a vulnerability warrants research on physical hardware, as the use of a simulation could not account for environmental noise, nor the accuracy of the sensor used by an eavesdropper. While the results obtained show that HD-QKD offer protection by increasing the number of dimensions an eavesdropper must measure, this also causes a reduced key efficiency as the number of potential encoding bases increase. Finally, the findings invite further investigation of a high-dimensional eavesdropping attack on entanglement based QKD algorithms such as E91 as a means of protection from this attack.

## References

- Alhazmi, S., Kandel, P., Sabovik, J., Matondo-Mvula, N., & Elleithy, K. (2023). Mitigating man-in-the-middle attack using quantum key distribution. In *2023 IEEE long island systems, applications and technology conference (LISAT)* (pp. 1–6). doi: 10.1109/LISAT58403.2023.10179560
- Amellal, H., Hajjami, S. E., Kaushik, K., Chhabra, G., & Yadav, S. A. (2023). Quantum man-in-the-middle attacks on QKD protocols: Proposal of a novel attack strategy. In *2023 6th International conference on contemporary computing and informatics (IC3I)* (Vol. 6, p. 513–519). doi: 10.1109/IC3I59117.2023.10397711
- Barker, E. (2020). *Recommendation for key management: Part 1 - general* (Tech. Rep. Nos. NIST Special Publication (SP) 800-53, Rev. 4, Includes updates as of January 22, 2015). Gaithersburg, MD: National Institute of Standards and Technology. Retrieved from <https://csrc.nist.gov/pubs/sp/800/57/pt1/r5/final> doi: 10.6028/nist.sp.800-57pt1r5
- Bechmann-Pasquinucci, H., & Gisin, N. (1999). Incoherent and coherent eavesdropping in the six-state protocol of quantum cryptography. , *59*, 4238–4248. Retrieved from <https://link.aps.org/doi/10.1103/PhysRevA.59.4238> doi: 10.1103/PhysRevA.59.4238
- Bechmann-Pasquinucci, H., & Tittel, W. (2000). Quantum cryptography using larger alphabets. *Physical Review A*, *61*(6). Retrieved from <http://dx.doi.org/10.1103/PhysRevA.61.062308> doi: 10.1103/physreva.61.062308
- Bennett, C. H. (1992, 5). Quantum cryptography using any two nonorthogonal states. *Phys. Rev. Lett.*, *68*, 3121–3124. Retrieved from <https://link.aps.org/doi/10.1103/PhysRevLett.68.3121> doi: 10.1103/PhysRevLett.68.3121
- Bennett, C. H., & Brassard, G. (1984). Quantum cryptography: Public key distribution and coin tossing. , 175–179. Retrieved from <http://dx.doi.org/10.1016/j.tcs.2014.05.025> doi: 10.1016/j.tcs.2014.05.025
- Beullens, W. (2022). *Breaking rainbow takes a weekend on a laptop*. Cryptology ePrint Archive, Paper 2022/214. Retrieved from <https://eprint.iacr.org/2022/214>
- Bommi, R. M., Nalini, M., Vijayaraj, N., & Kinol, A. M. J. (2023). Enhancing quantum key distribution protocols with machine learning techniques. In *2023 Intelligent computing and control for engineering and business systems (ICCEBS)* (p. 1–4). doi: 10.1109/ICCEBS58601.2023.10448811
- Bouchard, F., Fickler, R., Boyd, R. W., & Karimi, E. (2017). High-dimensional quantum cloning and applications to quantum hacking. *Science Advances*, *3*(2), e1601915. doi: 10.1126/sciadv.1601915
- Bruß, D. (1998). Optimal eavesdropping in quantum cryptography with six states. , *81*, 3018–3021. Retrieved from <https://link.aps.org/doi/10.1103/PhysRevLett.81.3018> doi: 10.1103/PhysRevLett.81.3018
- Castrycck, W., & Decru, T. (2023). An efficient key recovery attack on SIDH. In C. Hazay & M. Stam (Eds.), *Advances in cryptology – eurocrypt 2023* (pp. 423–447). Cham: Springer Nature Switzerland.
- Cirq Developers. (2024). *Cirq*. Zenodo. Retrieved from <https://doi.org/10.5281/zenodo.11398048> doi: 10.5281/zenodo.11398048
- Costello, C. (2021). *The case for SIKE: A decade of the supersingular isogeny problem*. Cryptology ePrint Archive, Paper 2021/543. Retrieved from <https://eprint.iacr.org/2021/543>

- Council of the European Union, & European Parliament. (2016). General data protection regulation. (119), 1-88.
- Ding, J., & Schmidt, D. (2005). Rainbow, a new multivariable polynomial signature scheme. In J. Ioannidis, A. Keromytis, & M. Yung (Eds.), *Applied cryptography and network security* (pp. 164–175). Berlin, Heidelberg: Springer Berlin Heidelberg.
- Djordjevic, I. B., & Nafria, V. (2024). Classical coherent states based quantum information processing and quantum computing analogs. *IEEE Access*, *12*, 33569–33579. doi: 10.1109/ACCESS.2024.3370430
- Du, J. (2023). The discovery and development of imaginary number. , *38*, 174–179. Retrieved from <https://drpress.org/ojs/index.php/HSET/article/view/5803> doi: 10.54097/hset.v38i.5803
- Ekert, A. K. (1991). Quantum cryptography based on bell’s theorem. *Phys. Rev. Lett.*, *67*, 661–663. Retrieved from <https://link.aps.org/doi/10.1103/PhysRevLett.67.661> doi: 10.1103/PhysRevLett.67.661
- Franklin, J. M., Howell, G. E., Boeckl, K. R., Lefkovitz, N. B., Nadeau, E. M., Shariati, B., ... others (2020). *Mobile device security: Corporate-owned personally-enabled (COPE)* (Tech. Rep. No. NIST Special Publication (SP) 1800-21). National Institute of Standards and Technology. doi: <https://doi.org/10.6028/NIST.SP.1800-21>
- Heisenberg, W. (1983). The actual content of quantum theoretical kinematics and mechanics (National Aeronautics and Space Administration, Trans.). *Z. Physik*, *43*, 172-198. (Original work published 1927) doi: <https://doi.org/10.1007/BF01397280>
- Huang, J., Wang, Y., Wang, H., Li, Z., & Huang, J. (2009). Man-in-the-middle attack on BB84 protocol and its defence. In *2009 2nd IEEE international conference on computer science and information technology* (pp. 438–439). doi: 10.1109/ICCSIT.2009.5234678
- Idan, Y., & Didi, A. (2024). A review of quantum communication using high-dimensional hilbert spaces. *arXiv preprint arXiv:2402.01319*. doi: 10.48550/arXiv.2402.01319
- Iqbal, M., Ahmadian, M., Velasco, L., & Ruiz, M. (2023). Reliable quantum communication. In *2023 23rd International conference on transparent optical networks (ICTON)* (pp. 1–4). doi: 10.1109/ICTON59386.2023.10207324
- James, P., Laschet, S., Ramacher, S., & Torresetti, L. (2023). Key management systems for large-scale quantum key distribution networks. In *Proceedings of the 18th international conference on availability, reliability and security*. New York, NY, USA: Association for Computing Machinery. doi: 10.1145/3600160.3605050
- Jawad, T. A., Mahmood, A. N., & Hameed, A. N. (2023). Detecting man-in-the-middle attacks via hybrid quantum-classical protocol in software-defined networks. *Indonesian Journal of Electrical Engineering and Computer Science*, *31*(1), 205–211. doi: 10.11591/ijeecs.v31.i1.pp205-211
- Kose, B. O., Coskun, V., Capa, M. O., & Uluoz, H. (2024). Security mechanisms in hybrid environments: The case of token online application. In *2024 International congress on human-computer interaction, optimization and robotic applications (HORA)* (p. 1-5). doi: 10.1109/HORA61326.2024.10550745
- Lee, C., Sohn, I., & Lee, W. (2022). Eavesdropping detection in BB84 quantum key distribution protocols. *IEEE Transactions on Network and Service Management*, *19*(3), 2689-2701. doi: 10.1109/TNSM.2022.3165202
- Liliana, Z. (2019). Two, three and four dimensional BB84: A comparative analysis based on C# simulation. In *2019 Eighth international conference on emerging security technologies (EST)* (p. 1-5). doi: 10.1109/EST.2019.8806204

- Liu, Y.-K., & Moody, D. (2024). Post-quantum cryptography and the quantum future of cybersecurity. *Phys. Rev. Appl.*, *21*, 040501. Retrieved from <https://link.aps.org/doi/10.1103/PhysRevApplied.21.040501> doi: 10.1103/PhysRevApplied.21.040501
- Longa, P., Wang, W., & Szefer, J. (2021). The cost to break SIKE: A comparative hardware-based analysis with AES and SHA-3. In T. Malkin & C. Peikert (Eds.), *Advances in cryptology – crypto 2021* (pp. 402–431). Cham: Springer International Publishing.
- Müller, R., Bacco, D., Oxenløwe, L. K., & Forchhammer, S. (2023). Information reconciliation for high-dimensional quantum key distribution using nonbinary LDPC codes. In *2023 12th International symposium on topics in coding (ISTC)* (pp. 1–5). doi: 10.1109/ISTC57237.2023.10273570
- Nielsen, M. A., & Chuang, I. L. (2010). *Quantum computation and quantum information: 10th anniversary edition*. Cambridge University Press.
- Office of the Federal Register, & National Archives and Records Administration. (1996). Health insurance portability and accountability act of 1996. In *Public law 104 - 191*. U.S. Government Printing Office.
- Qiskit contributors. (2023). *Qiskit: An open-source framework for quantum computing*. doi: 10.5281/zenodo.2573505
- Sabani, M., Savvas, I., Poulakis, D., & Makris, G. (2022). Quantum key distribution: Basic protocols and threats. In *Proceedings of the 26th pan-hellenic conference on informatics* (pp. 383–388). New York, NY, USA: Association for Computing Machinery. doi: 10.1145/3575879.3576022
- Saeed, M. H., Sattar, H., Durad, M. H., & Haider, Z. (2022). Implementation of QKD BB84 protocol in qiskit. In *2022 19th International bhurban conference on applied sciences and technology (IBCAST)* (p. 689-695). doi: 10.1109/IBCAST54850.2022.9990073
- Saki, A. A., Alam, M., Phalak, K., Suresh, A., Topaloglu, R. O., & Ghosh, S. (2021). A survey and tutorial on security and resilience of quantum computing. In *2021 IEEE european test symposium (ETS)* (p. 1-10). doi: 10.1109/ETS50041.2021.9465397
- Salas, C. J. R., & Barreto, D. F. M. (2024). *Quantum cryptography, BB84 protocol*. doi: 10.13140/RG.2.2.26217.67681
- Sasikumar, K., & Nagarajan, S. (2024). Comprehensive review and analysis of cryptography techniques in cloud computing. *IEEE Access*, *12*, 52325-52351. doi: 10.1109/ACCESS.2024.3385449
- Scarani, V., Acín, A., Ribordy, G., & Gisin, N. (2004). Quantum cryptography protocols robust against photon number splitting attacks for weak laser pulse implementations. *Phys. Rev. Lett.*, *92*, 057901. Retrieved from <https://link.aps.org/doi/10.1103/PhysRevLett.92.057901> doi: 10.1103/PhysRevLett.92.057901
- Shingari, N., & Mago, B. (2024). The importance of data encryption in ensuring the confidentiality and security of financial records of medical health. In *2024 IEEE international conference on interdisciplinary approaches in technology and management for social innovation (IATMSI)* (Vol. 2, p. 1-6). doi: 10.1109/IATMSI60426.2024.10503174
- Singh, G., Singh, A., & Sreenarayanan, N. M. (2022). Quantum cryptography with photon polarization and heisenberg uncertainty principle. In *2022 2nd International conference on advance computing and innovative technologies in engineering (ICACITE)* (pp. 1342–1346). doi: 10.1109/ICACITE53722.2022.9823504
- Sood, R., & Kaur, H. (2023). A literature review on RSA, DES and AES encryption algorithms. *Emerging Trends in Engineering and Management*, 57–63. doi: 10.56155/978-81-955020-3-5-

- Spranger, K. T., Grimaila, M. R., & Hodson, D. D. (2023). Understanding the quantum teleportation protocol. In *2023 Congress in computer science, computer engineering, & applied computing (CSCE)* (pp. 759–766). doi: 10.1109/CSCE60160.2023.00130
- Stratil, P., Hasegawa, S., & Shizuya, H. (2021). Supersingular isogeny-based cryptography: A survey. *Interdisciplinary Information Sciences*, *27*(1), 1-23. doi: 10.4036/iis.2020.R.02
- Wang, Y., Hu, Z., Sanders, B. C., & Kais, S. (2020). Qudits and high-dimensional quantum computing. *Frontiers in Physics*, *8*. Retrieved from <https://www.frontiersin.org/articles/10.3389/fphy.2020.589504> doi: 10.3389/fphy.2020.589504
- Wootters, W. K., & Zurek, W. H. (1982). A single quantum cannot be cloned. *Nature*, *299*(5886), 802–803. doi: 10.1038/299802a0
- Zahidy, M., Ribezzo, D., De Lazzari, C., Vagniluca, I., Biagi, N., Müller, R., ... Bacco, D. (2024). Practical high-dimensional quantum key distribution protocol over deployed multicore fiber. *Nature Communications*, *15*(1), 1651. Retrieved from <https://ntrs.nasa.gov/citations/19840008978> doi: 10.1038/s41467-024-45876-x
- Zi, W., Li, Q., & Sun, X. (2023). Optimal synthesis of multi-controlled qudit gates. In *2023 60th ACM/IEEE design automation conference (DAC)* (pp. 1–6). doi: 10.1109/DAC56929.2023.10247925

## A Reading Qudit Measurements in HD-Eavesdropping

Table 5: A table depicting the binary equivalent of a qudit measurement made by Bob and Eve when using BB84, wherein  $\rho$  is a random bit. Bob's binary values are only used in **Scenario 1**.

Measurement	Eve Binary	Bob Binary
0	0	0
1	0	$\rho$
2	1	1
3	1	$\rho$

Table 6: A table depicting the binary equivalent of a qudit measurement made by Bob and Eve when using the high-dimensional variant of BB84, wherein  $\rho$  are two random bits. Bob's binary values are only used in **Scenario 1**.

Measurement	Eve Binary	Bob Binary
0	00	00
1	00	$\rho$
2	01	01
3	01	$\rho$
4	10	10
5	10	$\rho$
6	11	11
7	11	$\rho$

Table 7: A table depicting the binary equivalent of a qudit measurement made by Bob and Eve when using SSP, wherein  $\rho$  is a random bit. Bob's binary values are only used in **Scenario 1**.

Measurement	Eve Binary	Bob Binary
0	0	0
1	0	$\rho$
2	0	$\rho$
3	1	1
4	1	$\rho$
5	1	$\rho$

## B Conversion Matrices

The unitary matrix for  $\text{QidConv}_1$ . This gate is used to convert four-dimensional qudits to qubits when analyzing BB84.

$$\begin{pmatrix} 1 & 0 & 0 & 0 & 0 & 0 & 0 & 0 & 0 & 0 & 0 & 0 & 0 & 0 & 0 & 0 \\ 0 & 1 & 0 & 0 & 0 & 0 & 0 & 0 & 0 & 0 & 0 & 0 & 0 & 0 & 0 & 0 \\ 0 & 0 & 1 & 0 & 0 & 0 & 0 & 0 & 0 & 0 & 0 & 0 & 0 & 0 & 0 & 0 \\ 0 & 0 & 0 & 1 & 0 & 0 & 0 & 0 & 0 & 0 & 0 & 0 & 0 & 0 & 0 & 0 \\ 0 & 0 & 0 & 0 & 0 & 1 & 0 & 0 & 0 & 0 & 0 & 0 & 0 & 0 & 0 & 0 \\ 0 & 0 & 0 & 0 & 1 & 0 & 0 & 0 & 0 & 0 & 0 & 0 & 0 & 0 & 0 & 0 \\ 0 & 0 & 0 & 0 & 0 & 0 & 0 & 1 & 0 & 0 & 0 & 0 & 0 & 0 & 0 & 0 \\ 0 & 0 & 0 & 0 & 0 & 0 & 1 & 0 & 0 & 0 & 0 & 0 & 0 & 0 & 0 & 0 \\ 0 & 0 & 0 & 0 & 0 & 0 & 0 & 0 & 0 & 0 & 1 & 0 & 0 & 0 & 0 & 0 \\ 0 & 0 & 0 & 0 & 0 & 0 & 0 & 0 & 0 & 0 & 0 & 1 & 0 & 0 & 0 & 0 \\ 0 & 0 & 0 & 0 & 0 & 0 & 0 & 0 & 1 & 0 & 0 & 0 & 0 & 0 & 0 & 0 \\ 0 & 0 & 0 & 0 & 0 & 0 & 0 & 0 & 0 & 1 & 0 & 0 & 0 & 0 & 0 & 0 \\ 0 & 0 & 0 & 0 & 0 & 0 & 0 & 0 & 0 & 0 & 0 & 0 & 0 & 0 & 0 & 1 \\ 0 & 0 & 0 & 0 & 0 & 0 & 0 & 0 & 0 & 0 & 0 & 0 & 0 & 0 & 1 & 0 \\ 0 & 0 & 0 & 0 & 0 & 0 & 0 & 0 & 0 & 0 & 0 & 0 & 0 & 1 & 0 & 0 \\ 0 & 0 & 0 & 0 & 0 & 0 & 0 & 0 & 0 & 0 & 0 & 0 & 1 & 0 & 0 & 0 \end{pmatrix}$$

The unitary matrix for  $\text{QidConv}_2$  is depicted below. This gate is used to convert eight-dimensional qudits to four-dimensional qudits when analyzing the high-dimensional variant of BB84.



